Mon. Not. R. astr. Soc. (1985) **212**, 737–749

The intensities of the sulphur III lines and the ionization mechanisms in Liners

Angeles I. Díaz *Astronomy Centre, University of Sussex, Falmer, Brighton, East Sussex BN1 9QH*

B. E. J. Pagel and I. R. G. Wilson *Royal Greenwich Observatory, Herstmonceux Castle, Hailsham, East Sussex BN27 1RP*

Accepted 1984 September 24. Received 1984 September 24; in original form 1984 July 4

Summary. New near-infrared spectrophotometric observations show that the relative strengths of the sulphur emission lines [S III] λλ 9069, 9532 Å with respect to Hα constitute a powerful diagnostic to distinguish between shock and photoionization mechanisms in Liners. These observations strongly support the idea, already favoured on the basis of abundance arguments, that Liners and Seyferts form a continuous sequence, both types of objects being photoionized, but with the ionization parameter being lower in Liners. This photoionization could be due either to the presence of a central nonthermal source or to recent star formation.

1 Introduction

Weak emission-line activity is present in the nuclei of many early-type galaxies (Stauffer 1982; Keel 1983). The dominant form of this nuclear emission exhibits characteristics sufficiently different from those of Seyfert and H II region nuclei as to constitute a distinct class of objects that are referred to as Liners (Heckman 1980).

The word Liner stands for *L*ow *I*onization *N*uclear *E*mission-line *R*egion and essentially applies to an active nucleus whose spectrum is dominated by low-excitation lines. Liners show moderately strong [O III] emission with [O III] λ 5007/Hβ ≃ 3, compared to a ratio of 10 or more in Seyfert 2s and the narrow-line regions of Seyfert 1s, and a ratio of less than one in the high-abundance nuclear H II regions. Liners also have a large (N II] λ 6584/Hα ratio which is typically of the order of unity or greater. Liners differ from Seyferts in having lower emission-line luminosities, but both types of objects possess a number of similar features. Typical emission-line widths in Liner spectra are greater than 300 km s^{-1}, comparable to the velocity dispersions observed in Seyfert 2s and distinctly larger than those measured in nuclear H II regions. Some Liners also show a broad component of Hα and/or X-ray emission suggesting the presence of nuclear activity akin to that in Seyferts. However, the contribution of a featureless continuum characteristic of these latter objects, which leads to the assumption of a nonthermal origin for their activity, is lacking in most Liners, in which the continuum is dominated by starlight.

The excitation mechanism which produces the distinctive Liner spectrum has been a topic of considerable interest in recent years. Initially, Heckman (1980) and Baldwin, Phillips & Terlevich (1981) attributed the excitation mechanism to shock-wave heating, on the basis of many similarities found between the optical spectra of Liners and shock-heated gas (e.g. supernova remnants). But subsequent work by Ferland & Netzer (1983), Halpern & Steiner (1983) and Péquignot (1984) has shown that it is possible to reproduce the observed emission-line ratios in Liners if the emitting gas is assumed to be photoionized by a power-law continuum similar to that assumed for Seyfert 2s (i.e. $F_\nu \propto \nu^{-1.5}$) but with a lower ionization parameter (ratio of ionizing photons at the Lyman continuum to the electron density), thus suggesting that a continuous sequence of power-law ionizing radiation with decreasing ionization parameter can explain the emission-line spectra of Seyfert 2s and Liners.

The most striking feature common to the optical spectra of Liners is the large strength of the [N II] λλ6548, 6584 lines relative to Hα, initially taken as an indication for the existence of nitrogen over abundances in these nuclei (e.g. Peimbert 1968). Indeed, if Liner and Seyfert emission-line spectra are assumed to be produced by different mechanisms, shock-wave heating and power-law photoionization respectively, then, in order to explain the [N II] λ6584 and [O III] λ5007 line-strengths, the nitrogen abundance is required to increase steadily from high-excitation objects to low-excitation objects by up to a factor of three. On the other hand, the power-law excitation sequence can explain the line ratios observed in Seyferts and Liners with constant and quite plausible abundances (i.e. solar or slightly over solar). These abundances are in agreement with those deduced from observations of H II regions surrounding these nuclei (Pagel 1984; Phillips *et al.* 1984).

The strengths of some weak lines, in particular [O III] λ4363 and He II λ4686, have been proposed as possible diagnostics to distinguish between shock heating and power-law photoionization mechanisms. Very high electron temperatures as deduced from the λ4363/λ5007 ratio of [O III] would rule out photoionization. There are two problems, though, which preclude the use of the [O III] λ4363 line as a diagnostic in Liners. Firstly, the line is intrinsically faint, making it difficult to measure against a strong underlying continuum cut up by stellar absorption lines. Its proximity to the strong Hγ line worsens the situation. Secondly, the λ4363/λ5007 ratio is enhanced in some Liners by collisional de-excitation of λ5007 at high densities, making this ratio useless as a temperature indicator (Carswell *et al.* 1984).

The He II λ4686 line constitutes a more promising diagnostic, as its intensity is essentially dependent on the spectral energy distribution of the ionizing radiation. Power-law photoionization models predict the He II λ4686/Hβ ratio to have a very restricted range of values (Stasińska 1984a, b), whereas the ratios observed in Seyfert 2s and Liners cover a range which is substantially greater. In order to reproduce the different He II line strengths observed in Seyfert 2s, Stasińska (1984b) has suggested that these objects may be photoionized by a spectrum resembling that of a blackbody at a temperature greater than 150 000 K. By extension, this conclusion might also apply to Liners. This blackbody-like spectrum can be produced by thermal processes such as accretion-disc emission (Péquignot 1984; Malkan & Sargent 1982), but it could also be due to recent star formation (Terlevich & Melnick 1984). According to recent studies of stellar evolution (Maeder 1983), high-mass stars may suffer very large mass losses, at rates strongly dependent on metallicity, exposing their carbon–oxygen cores at the end of their lifetimes and reaching effective temperatures of the order of 2×10^5 K. Stellar clusters which are sufficiently old to contain a significant number of these objects (called 'Warmers' by Terlevich & Melnick 1984) would give rise to an ionizing spectrum that can adequately reproduce the spectra of Liners and, in particular,

explain the differences in the He II λ 4686/Hβ ratio. Therefore, if it can be shown conclusively that shock-heating is not the dominant ionization mechanism acting in Liners, this would open the door to the very interesting possibility that the high excitation observed in these nuclei could be the result of violent star-formation activity in regions of high metal abundance.

The intensities of the [S III] λλ 9069, 9532 nebular emission lines can provide a powerful additional diagnostic. Theoretical models predict quite distinct behaviours of these lines in shock and photoionization regimes, and it is actually possible to distinguish among the various ionization mechanisms if complementary observations of the oxygen emission-line intensities are used. In this paper we present spectrophotometric observations covering the spectral range λλ 5800–10050 Å of four Liners and one Seyfert 2 nucleus for which optical observations already exist. The ionization mechanisms are then discussed in the light of the results obtained from them.

2 Observations

The observations discussed in this paper were made at the AAT using the RGO spectrograph and the RGO CCD (an RCA SID 53612 back-illuminated thin chip, Jorden, Thorne & van Breda 1982). The CCD has a readout noise of ~ 70 electrons per pixel, an array size of 320 × 512 pixels, and a pixel size of 30 μm^2. All observations were made with a 220-μm slit (projecting to 1.5 arcsec on the sky) and no decker. The projected slit length was 4.9 arcmin, the limits being set by the physical size of the CCD chip (320 pixels), and the projected pixel size in the spatial direction was 0.93 arcsec. Using a dispersion of approximately 4.3 Å pixel^{-1}, we observed the spectral region from λ 5800 to λ 10 050 Å in three overlapping sections of 2100 Å each. The three spectral ranges were: λλ 5800–7900, 7050–9150 and λλ 8000–10 100 Å. In total, four Liners, NGC 1097, 1672, 1433 and 7590, and one Seyfert galaxy, NGC 1365, were observed on the nights of 1983 October 21 and 22. Large H II regions close to the nuclei of the programme galaxies were also observed.

NGC 1097 is a southern barred spiral galaxy which looks peculiar in several respects: it possesses a 'hotspot' nucleus, seems to be interacting with a close companion, and has optical jets. Its nucleus displays a strong optical continuum dominated by late-type stars and broad (~ 500 km s^{-1}) emission lines whose relative strengths place it among the classic Liners (see Phillips *et al.* 1984 and references therein). A weak compact radio source is associated with it (Wolstencroft, Perley & Tully 1984).

NGC 1433 is another southern barred spiral whose nucleus has been classified by Sérsic & Pastoriza (1965) as 'amorphous' and it also shows Liner-like emission (Pagel 1984).

NGC 1672 can also be found in Sérsic & Pastoriza's (1965) list of galaxies with peculiar nuclei. Although the relative strengths of its nuclear emission lines are close to those found in H II regions (Osmer, Smith & Weedman 1974), the [O III] lines are much broader than Hβ (Véron, Véron & Zuiderwijk 1981), and the ratio of [O III]/Hβ is slightly greater than 1 (Díaz, in preparation). The radio source PKS 0444–593 has been identified with this galaxy (Wright, Savage & Bolton 1977) and it has also been detected as an X-ray source by the *Einstein Observatory* (Griffiths, Feigelson & van Speybroeck 1979).

NGC 7590 is an intermediate spiral (SAbc; Shobbrook 1966) belonging to the Grus quartet which also contains the X-ray Seyfert galaxy NGC 7582 and the starburst galaxy NGC 7552 (Ward *et al.* 1980). It forms a pair with NGC 7599 and has been reclassified as SAc by Sandage & Brucato (1979). It has also been classified as a Liner by Pagel (1984).

NGC 1365 has been included in this study as an example of a nearby Seyfert galaxy. Its nuclear spectrum has been studied in great detail by Alloin *et al.* (1981), Edmunds & Pagel (1982) and Phillips *et al.* (1983).

Table 1. Objects observed.

Object	(1950.0)		PA degrees	Columns
	hr m s	° ′ ″		
N1672SE	04 44 55	−59 20 12	57	116–128
N1672NUC	04 44 55	−59 20 12		126–128
N1672NW	04 44 55	−59 20 12		139–147
N1097NE	02 44 11	−30 29 06	140	114–127
N1097NUC	02 44 11	−30 29 06		128–135
N1097SW	02 44 11	−30 29 06		136–149
N1433NUC	03 40 27	−47 22 48	120	127–136
N7590NUC	23 16 11	−42 30 42	150	130–137
N1365SY*	03 31 42	−36 18 27	180	120–125
N1365NUC	03 31 42	−36 18 27		124–127
N1365N	03 31 42	−36 18 27		101–113
LTT 9239	22 51 53	−20 40 15	–	124–146

* Coordinates of the Seyfert nucleus. The slit centre was placed 9 arcsec to the north of the nucleus.

Details of the observations are listed in Table 1. NUC, NE (NW) or SW (SE) following the NGC number of the object designates nucleus, H II region north-east (west) from the nucleus or H II region south-west (east) from the nucleus respectively. Three entries are given for NGC 1365: one for the Seyfert nucleus, designated by Sy, a second for the nebulosity underlying the nucleus, referred to as NUC and a third for a nuclear H II region to the north of the nucleus, designated by N. The position angles of the observations are listed in column 4. These were chosen to match previous optical observations. Column 5 gives the channels of the CCD detector which were added together to form the output spectra (see Section 3). The coordinates given in columns 2 and 3 of Table 1 correspond to channel number 132.

3 Reductions

The data reduction was carried out at the RGO STARLINK node using a combination of the standard ASPIC software and the SPICA spectral reduction package. The data reduction procedure included:

(1) removal of the dc bias,
(2) division by a flat-field frame,
(3) sky subtraction,
(4) extraction of spectra and compression to one dimension,
(5) wavelength calibration,
(6) correction for atmospheric extinction,
(7) merging of the three wavelength regions.

The orientation of the CCD chip was arranged so that the dispersion was parallel to readout direction, removing the need to do a full two-dimensional wavelength calibration. The accuracy of the wavelength fit was roughly a quarter of a channel (~ 1 Å) over the full spectrum.

Severe fringing, producing a 50 per cent modulation of the data, was successfully removed by dividing the data frame by a flat-field frame. Residual fringing remained in particular regions of the chip, affecting the reduced spectra for wavelengths shortward of 6300 Å and longward of 9700 Å. Features in these spectral ranges should be treated as suspect.

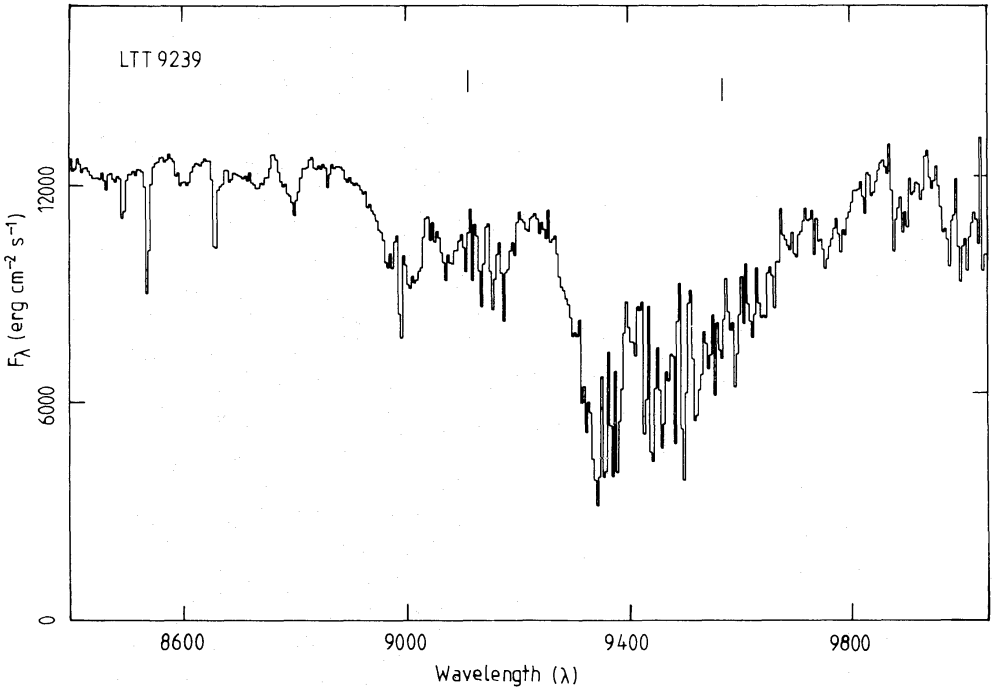

Figure 1. The atmospheric absorption features in the spectrum of the standard star LTT 9239. The wavelengths of the [S III] λλ 9069, 9532 lines are marked to show their positions relative to the underlying atmospheric absorption bands. A redshift of 1000 km s^{-1}, typical of the Liner galaxies observed, has been applied.

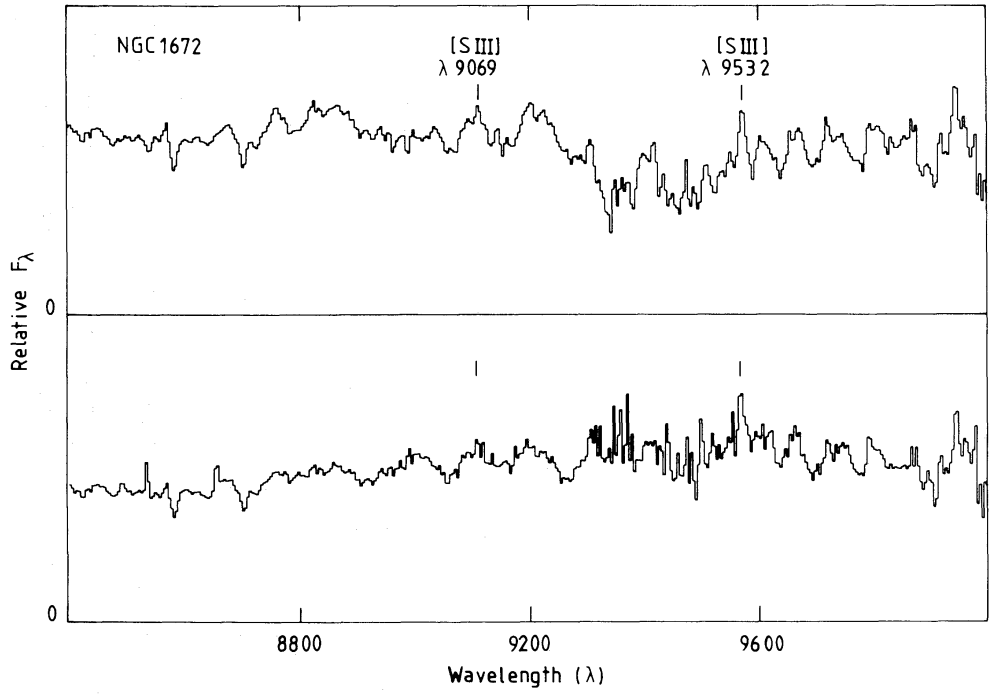

Figure 2. The far-red spectrum of the Liner nucleus in NGC 1672, before (top) and after (bottom) division by the spectrum of the standard star LTT 9239. The positions of the [S III] λλ 9069, 9532 lines are shown redshifted to the galaxy's rest-frame. Division by the featureless spectrum of a standard star appears to be successful in removing low-frequency atmospheric spectral features, although it is unable to correct completely for the strong narrow water-vapour lines in the λλ 9300–9500 wavelength region.

Fig. 1 shows the atmospheric absorption features present in the observed wavelength range. The regions around both the [S III] λλ 9069 and 9532 lines are heavily cut up by atmospheric water-vapour absorption bands, which must be removed in order to determine the strengths of the sulphur lines. In our reduction procedure, each of the spectra had the low-frequency atmospheric extinction removed using a mean extinction curve applicable to the Siding Spring observing site (Fosbury, private communication). Two methods were then used to remove the higher frequency atmospheric spectral features. The first was to divide the object spectrum by that of standard star LTT 9239, one of the group of southern hemisphere spectrophotometric standards published by Stone & Baldwin (1983) and Baldwin & Stone (1984), with a relatively featureless continuum and calibrated fluxes out to λ 10 400 Å. Fig. 2, showing the spectrum of NGC 1672 before and after division by the standard, indicates how effective this technique is in removing the absorption bands. It is evident that only the relatively low frequency spectral features are successfully removed, while the narrow saturated water-vapour absorption lines (evident in the λλ 9300–9500 spectral region) are not. In view of saturation effects this is not surprising. The second method, more suitable for saturated-line removal, was based on the standard spectrum being normalized to the local object continuum and then subtracted from the galaxy spectrum. This method can only be used over a limited spectral region (~ 500 Å at most), and assumes that the atmospheric absorption lines have a constant relative depth compared to the continuum. The technique will not work if the atmospheric absorption lines are varying in intensity with time and/or position on the sky, or if there is an atmospheric absorption component in the lines which is a non-linear function of the air-mass. We do not consider the latter effect to be a problem for our observations, as all the objects (including the standard star) were observed within 20° of the zenith, except NGC 1672 which was observed at 30°. The second method was only marginally better than the first and therefore we have divided all spectra by the spectrum of the standard star, since we believe that this gives us a truer picture of the continuum under-

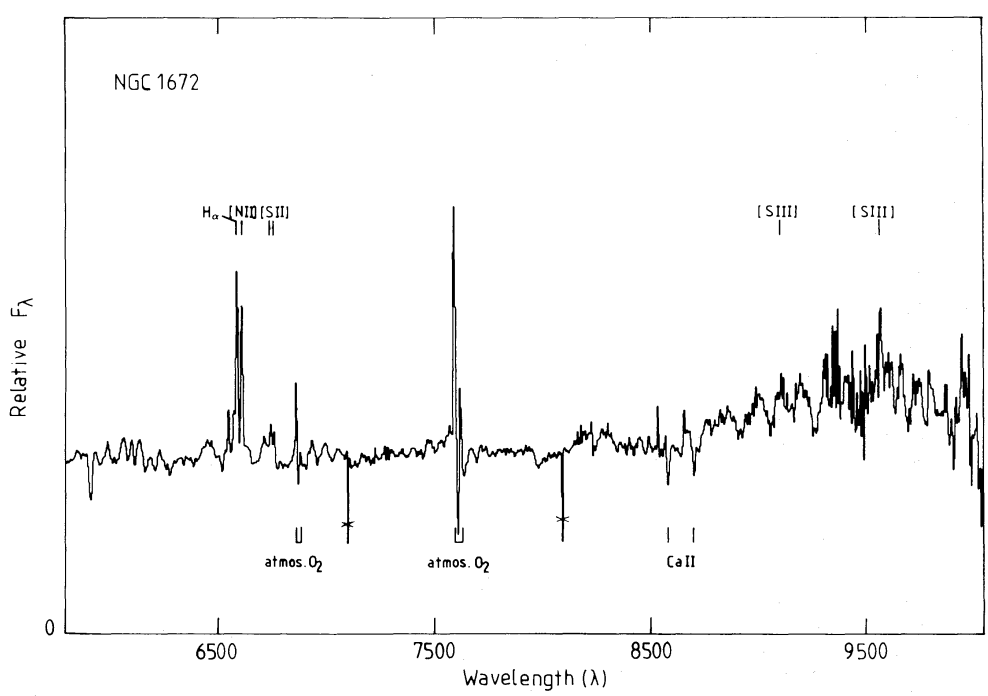

Figure 3. Final merged spectrum of NGC 1672. Crosses mark the glitches produced by the merging of the three spectral regions.

lying the [S III] emission lines. Fig. 3 shows the final merged spectrum of the nucleus of NGC 1672.

The [S III] line intensities were measured by fitting a polynomial function to the local continuum, subtracting it from the spectrum and then determining the residual intensity in a 20-Å bin centred on the nominal wavelength of the [S III] lines in the rest frame of the galaxy. The continuum used covered roughly 40 to 60 Å on either side of the nominal position of the lines. Estimates of the formal internal errors in the line intensity ratios were determined from the rms noise of the continuum and the photon noise in the line, the first being by far the largest source of uncertainty. External errors can only be determined from repeated observations and are probably much larger than the quoted ones.

4 Results

The [S III] lines were detected in the nuclei and nuclear H II regions of NGC 1097, 1672 and 1365. They were also detected in the nucleus of NGC 7590, although only at the 3σ level. No lines were detected in the nucleus of NGC 1433, for which only upper limits (set at the 3σ level of the underlying continuum) could be obtained. Fig. 4 shows the reduced spectra of the nuclei of NGC 1672 and 1097 in the spectral range λ 8400 to λ 10 000 Å. The two galaxies have very similar redshifts (1309 and 1320 km s^{-1} respectively) which allows a straightforward comparison of both spectra. [S III] λ 9532 can be seen in the nucleus of NGC 1097 although there is no sign of the λ 9069 line. This is not surprising if we allow for the fact that the λ 9069 line is at least 2.44 times weaker than the λ 9532 line, and take into

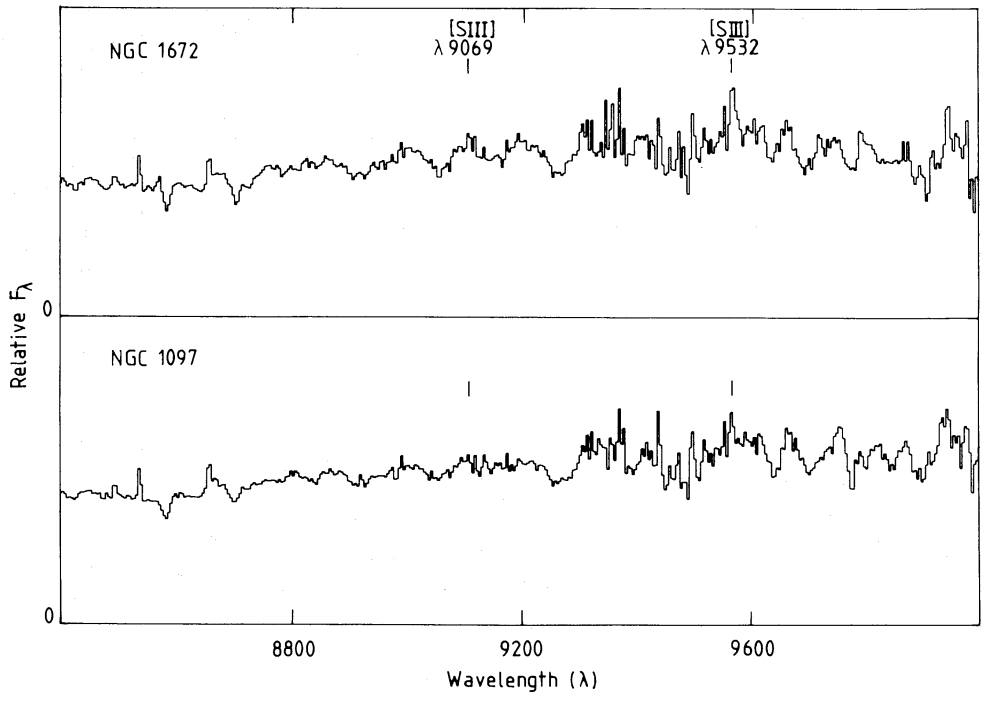

Figure 4. The far-red spectra of the Liner nuclei NGC 1672 and 1097. Both galaxies have very similar redshifts (1309 and 1320 km s^{-1} respectively) amounting to less than $^1/_{10}$ of a channel shift for the rest frames of the two galaxies, allowing direct comparison of spectral features between the two spectra. Intercomparison of the spectra shows that the red [S III] line is clearly present in the spectrum of NGC 1097 though the blue line is not evident. This is not surprising considering the fact that it is more than 2.4 times fainter than the red line.

account the cut-up nature of the underlying continuum. It should be emphasized that the [S III] λ9532 line in our programme galaxies has been redshifted out of the spectral region worst affected by the atmospheric absorption bands (i.e. from 9300 to 9500 Å; see Fig. 1) and is still blueward of the region affected by residual fringing redward of 9600 Å.

Table 2 lists the dereddened [S III] λλ9069, 9532 and [S II] λλ6716, 6731 line intensities for the programme objects relative to Hα. For the Seyfert nucleus of NGC 1365 it was not possible to resolve the narrow component of Hα. The [S III]/Hα ratio was therefore obtained from the observed [S III]/[S II] ratio of 0.68 and the [S II]/Hα ratio given by Alloin *et al.* (1981) for the narrow-line region. Also listed are the ratios [S II] λλ6716, 6731/Hα, [O III] λλ4959, 5007/Hβ and [O II] λ3727/Hβ derived from optical spectra obtained from the references cited in column 8. The Hα/Hβ ratios measured on these same spectra were used to determine the value of the reddening constants given in column 7. The line-intensity ratios were then corrected for reddening by assuming a theoretical value for the Balmer decrement corresponding to case B recombination (Brocklehurst 1971). In the cases in which measures of the [O III] λ4959 line strength were not given, a ratio of [O III] λ5007/λ4959 = 3.0 was assumed. For the nuclear region of NGC 1672, no measures of the

Table 2. Reddening-corrected line intensity ratios.

Object	[S III]/Hα	[S II]/Hα[a]	[S II]/Hα Opt	[O III]/Hβ	[O II]/Hβ	c	Ref
N1672SE	0.24[a]	0.27	–	–	–	–	–
N1672NUC	0.24[b]	0.30	–	1.29	–	–	2
N1672NW	0.11[a]	0.20	–	–	–	–	–
N1097NE	0.08[b]	0.16	0.13	0.13	0.50	1.4	1
N1097NUC	0.86[c]	0.84	0.94	3.97	6.12	0.9	1
N1097SW	0.16[b]	0.22	0.21	0.17	1.05	1.6	1
N1433NUC	⩽0.34	1.20	0.82	4.01	3.89	0.48	2
N7590NUC	0.47[c]	0.99	0.74	4.83	2.57	0.36	2
N1365SY	0.05	–	0.16	3.50	0.70	1.00	3
N1365NUC	0.23[a]	0.18	0.17	1.57	2.19	1.50	4
N1365N	0.41[b]	0.21	–	–	–	–	4

Uncertainty: a ⩽10 per cent, b ⩽ 20 per cent, c ⩽ 30 per cent.

1. Phillips *et al.* 1984.
2. Díaz, in preparation.
3. Alloin *et al.* 1981.
4. Edmunds & Pagel 1982.

[O II] line strengths were available. A lower limit to the ratio of [O II]/[O III] was set under the assumption that a ratio of [O III]/Hβ < 3 for Liners implies a ratio of [O II]/[O III] > 1 (Baldwin *et al.* 1981). The [S II]/Hα ratios derived from the optical spectra (column 4) are in excellent agreement with those obtained from the CCD observations, considering the quoted error of 10–20 per cent for the optical results.

5 Discussion and conclusions

Figs 5 and 6 show the positions of the observed objects on the excitation diagrams [S II] λλ6717, 6731/Hα versus [S III] λλ9069, 9532/Hα and [S II] λλ6717, 31/[S III] λλ9069, 9532 versus [O II] λλ3726, 29/[O III] λλ4959, 5007 in logarithmic form, together with theoretical models and the available data on H II regions in the Galaxy and the

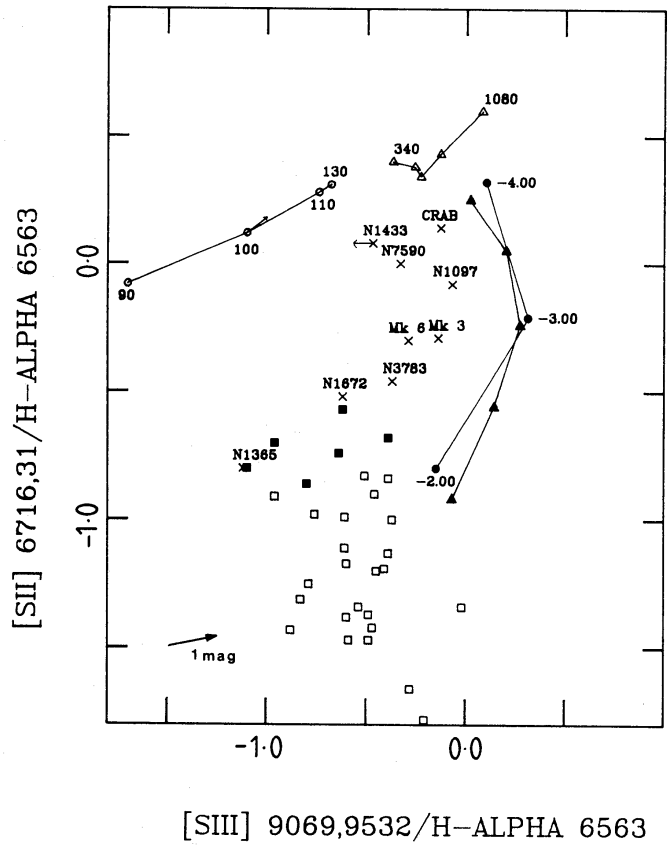

Figure 5. Logarithmic line intensity ratios [S II]/Hα versus [S III]/Hα. Details of the figure are given in the text.

Magellanic clouds. Although in principle it would be more convenient to take intensity ratios with only λ6731, which is less sensitive to collisional de-excitation, both lines of [S II] $\lambda\lambda$6717, 6731 have been used together, since they were only partially resolved in our data. We do not consider this to be a serious problem since the mentioned effect only begins to be important at densities of the order of $10^4\,\mathrm{cm}^{-3}$.

The theoretical models are shown as symbols connected by straight lines. Open circles correspond to the self-consistent shock models of Shull & McKee (1979). Only the models with high shock-velocities have been plotted, since the rest of them produce intensities of [S III] and [O II] which are too small and too large respectively to fit the observations. For all these models the pre-shock density is taken to be $N = 10\,\mathrm{cm}^{-3}$. The small arrow at the point corresponding to a shock velocity of $100\,\mathrm{km\,s}^{-1}$ shows the effect of increasing the density for this model by a factor of 10. Open triangles in the diagrams represent models of steady-state high-velocity shocks (ranging from 340 to $1080\,\mathrm{km\,s}^{-1}$) propagating through a low-density medium ($N = 10\,\mathrm{cm}^{-3}$) computed by Binette, Dopita & Tuohy (1984). All the shock models shown correspond to solar abundances and are labelled according to their shock velocity.

Power-law photoionization models (Stasińska 1984a) are shown as filled circles. Models of spectral index $\alpha = -1.5$, particle density $N = 10^3\,\mathrm{cm}^{-3}$ and solar composition are plotted following a sequence of decreasing ionization parameter, U, from 10^{-2} to 10^{-4}. Raising the metallicity to a value of twice solar moves the points left and down in Fig. 5 by ~ 0.1 dex. An increase in density from 10^2 to $10^3\,\mathrm{cm}^{-3}$ in the solar composition model produces a negligible shift in the curve. At higher densities (~ $10^4\,\mathrm{cm}^{-3}$), [S II] begins to become colli-

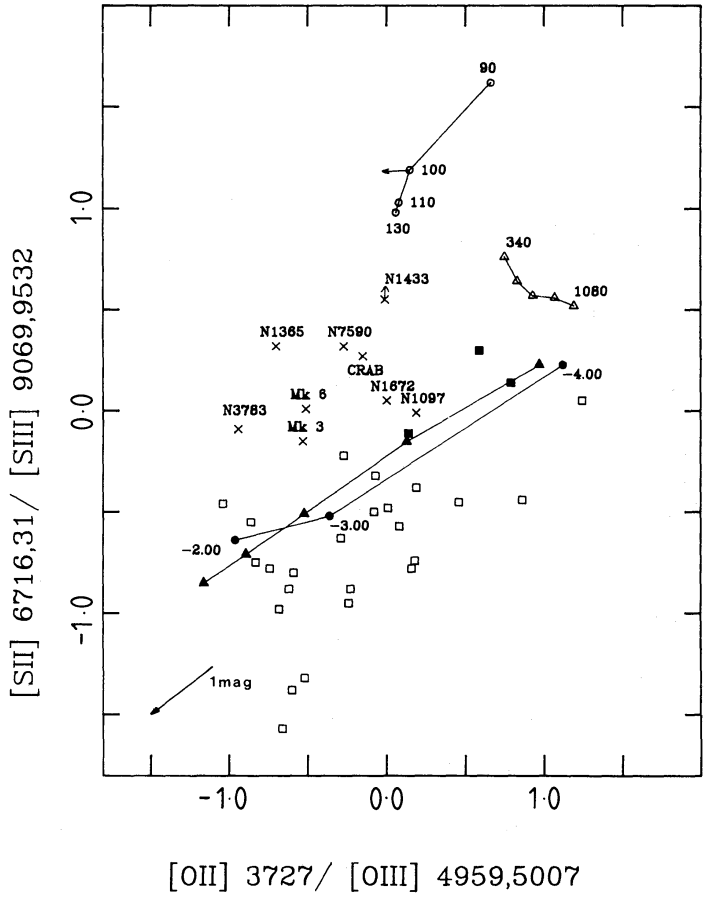

Figure 6. Same as for Fig. 5 but for [S II]/[S III] versus [O II]/[O III].

sionally de-excited and the [S II]/Hα ratio drops by more than a factor of three. At higher metallicities this effect is less dramatic.

Finally, filled triangles correspond to models of photoionization by young stellar clusters of solar composition for which the effects of strong mass-loss in the evolution of their high-mass stars have been taken into account (Terlevich & Melnick 1984). The models correspond to an age of 3×10^6 yr, by which time the highest mass stars in the clusters have reached the Warmer stage, and are computed for different cluster sizes. The models are parameterized according to the ionization parameter, U, in order to facilitate the comparison with power-law photoionization models. The atmospheres of Warmers are taken to be composed of pure helium and have a high surface gravity and an average effective temperature of 170 000 K. An initial mass function similar to the one observed in the solar neighbourhood for high-mass stars (Lequeux 1980) was assumed for the clusters. All photoionization models are labelled according to the logarithm of their ionization parameter.

Our data are shown as filled squares for nuclear H II regions and crosses for the actual galactic nuclei. Individual objects are labelled. Also included in the diagrams are the data corresponding to the narrow-line regions of three Seyfert galaxies: Mk 3 and Mk 6 (Malkan & Oke 1983) and NGC 3783 (Ward & Morris 1984). In the case of Mk 6 the ratio between the broad and narrow components of Hα reported by Koski (1978) has been used. Open squares correspond to normal H II regions both in the Galaxy and in the Magellanic clouds (Dennefeld & Stasińska 1983) and are shown in order to represent the locus of objects photoionized by hot OB stars. The position of a bright filament in the Crab Nebula, studied

by Dennefeld & Péquignot (1983) and Péquignot & Dennefeld (1983) and well-fitted by power-law photoionization models, is also shown. These additional data have been corrected for reddening in the same way as our own data and the reddening vector is shown at the bottom left corner of the diagram.

Perhaps the most remarkable feature of the [S II]/Hα versus [S III]/Hα diagram (Fig. 5) is the clear separation between the H II regions and Liner nuclei, except in the case of NGC 1672 which has properties characteristic of both Liners and starbursts. This object has a bluer continuum than the rest of the Liners in our sample (Osmer *et al.* 1974) and shows broad Balmer absorption wings (Véron *et al.* 1981). In this diagram, Seyfert nuclei and Liners seem to follow a sequence parallel to the one defined by photoionization models with decreasing ionization parameter, but somewhat shifted to the left. Bearing in mind the necessary oversimplification of the theoretical models, as evidenced by the position of the Crab filament point in the diagram, all the Liner nuclei are consistent with models of photoionization with a low ionization parameter, except in the case of NGC 1672, for which a higher ionization parameter should be invoked unless its spectrum is heavily contaminated by H II regions. The photoionization could be produced either by a central nonthermal source or by a young stellar cluster with Warmers, but contributions from shocks cannot be ruled out, especially in the case of NGC 1433 for which the datum point shown represents only an upper limit to the [S III]/Hα ratio.

The second diagram, [S II]/[S III] versus [O II]/[O III] (Fig. 6), does not allow a distinction between different types of photoionization mechanism (hot OB stars, power-law spectrum or young star cluster with Warmers), but it does seem to constitute a good diagnostic between these and the shock models, since the lower ionization stages are enhanced in the shock-heating case with respect to power-law photoionization models. In this diagram Seyferts and Liners also show a tendency to lie parallel to the photoionization sequence, although the scatter in this case is rather high and cannot be attributed purely to observational errors. Again, uncertainties in the models could be responsible for the scatter, especially if charge-exchange reactions between S^{2+} and either H or He are present, as suggested by Dennefeld & Péquignot (1983), thus enhancing [S II] over [S III]. This does not alter the fact that all our nuclei are far from the region of the diagram where shock models lie, and are close to the position of the Crab filament point. Thus we think it is possible to discriminate between the shock heating and photoionization mechanisms if both diagrams are used simultaneously.

Our data nevertheless suggest that Liners are far from being a homogeneous class of objects. If we assume that several excitation mechanisms are actually at work in Liners, the positions of the different objects in the [S II]/Hα versus [S III]/Hα diagram would show the results of different contributions from each mechanism, shock-heating processes becoming increasingly significant along the sequence defined by NGC 1097, 7590 and 1433, and a blackbody component, probably resulting from the contribution of a young stellar population, being important in the case of NGC 1672. If Liners are assumed to be photoionized by a power-law spectrum similar to the one operative in Seyferts, the position of this latter object can only be explained as the result of contamination by nearby H II regions which, of course, cannot be excluded. Such contamination was, indeed, demonstrated by Véron *et al.* (1981) for their data, but it could be less significant for the smaller aperture used in the present investigation. On the other hand, if the pseudo-activity of Liners is linked solely to nuclear star-formation processes, then the different Liner subtypes might correspond to different evolutionary stages of the region surrounding the starburst or even represent the results of different evolutionary patterns. Terlevich & Melnick (1984) actually predict two different evolutionary sequences depending on the size of the starburst. A large one would

first produce a low-excitation H II region which would then subsequently evolve to a Seyfert 2 type nucleus and later to a 'blue' Liner, i.e. a Liner whose spectrum shows some evidence of an underlying blue continuum and, probably, some features revealing the presence of young stars, as in the case of NGC 1672. Liners in which the blue optical continuum of the young stellar cluster is practically undetectable and whose optical continua are dominated by an old stellar population ('red' Liners) would be the result of the evolution of the low-excitation H II regions surrounding small starbursts. Objects like NGC 1433, 1097 and 7590 would fall under this second category. Since small bursts are probably more frequent than large ones, it should not be surprising that only one of the Liners in our sample shows 'blue' Liner characteristics.

Obviously, more and better quality data similar to the ones presented in this study are needed in order to decide among these various possibilities.

Acknowledgments

We thank John Lucey and the AAT staff for their assistance during the observations, especially with the RGO CCD detector, and Roberto Terlevich for very helpful discussions and for providing information about the Terlevich & Melnick (1984) paper in advance of publication. One of the authors, Angeles Díaz, acknowledges the receipt of a Vicente Cañada Blanch Foundation Fellowship, administered through the British Council, and an Overseas Research Student Award.

References

Alloin, D., Edmunds, M. G., Lindblad, P. O. & Pagel, B. E. J., 1981. *Astr. Astrophys.*, **101**, 372.
Baldwin, J. A., Phillips, M. M. & Terlevich, R., 1981. *Publs astr. Soc. Pacif.*, **93**, 5.
Baldwin, J. A. & Stone, R. P. S., 1984. *Mon. Not. R. astr. Soc.*, **206**, 241.
Binette, L., Dopita, M. A. & Tuohy, I. R., 1984. *Astrophys. J.*, submitted.
Brocklehurst, M., 1971. *Mon. Not. R. astr. Soc.*, **153**, 471.
Carswell, R. F., Baldwin, J. A., Atwood, B. & Phillips, M. M., 1984. Preprint.
Dennefeld, M. & Péquignot, D., 1983. *Astr. Astrophys.*, **127**, 42.
Dennefeld, M. & Stasińska, G., 1983. *Astr. Astrophys.*, **118**, 234.
Edmunds, M. G. & Pagel, B. E. J., 1982. *Mon. Not. R. astr. Soc.*, **198**, 1089.
Ferland, G. J. & Netzer, H., 1983. *Astrophys. J.*, **264**, 605.
Griffiths, R. E., Feigelson, E. & van Speybroeck, L., 1979. *Bull. Am. astr. Soc.*, **11**, 466.
Halpern, J. P. & Steiner, J. E., 1983. *Astrophys. J.*, **269**, L37.
Heckman, T. M., 1980. *Astr. Astrophys.*, **87**, 152.
Jorden, P. R., Thorne, D. J. & van Breda, I. G., 1982. *Soc. Photoopt. Instr. Eng.*, **331**, 87.
Keel, W. C., 1983. *Astrophys. J. Suppl.*, **52**, 229.
Koski, A. T., 1978. *Astrophys. J.*, **223**, 56.
Lequeux, J., 1980. *Star Formation*, eds Maeder, A. & Martinet, J., p. 77, Geneva Observatory publication.
Maeder, A., 1983. *Astr. Astrophys.*, **120**, 113.
Malkan, M. A. & Oke, J. B., 1983. *Astrophys. J.*, **265**, 92.
Malkan, M. A. & Sargent, W. L. W., 1982. *Astrophys. J.*, **254**, 22.
Osmer, P. S., Smith, M. G. & Weedman, D. W., 1974. *Astrophys. J.*, **192**, 279.
Pagel, B. E. J., 1984. *The Formation and Evolution of Galaxies and Large Structure in the Universe*, p. 437, eds Audouze, J. & Van, J. T. T., Reidel, Dordrecht, Holland.
Peimbert, M., 1968. *Astrophys. J.*, **154**, 33.
Péquignot, D., 1984. *Astr. Astrophys.*, **131**, 159.
Péquignot, D. & Dennefeld, M., 1983. *Astr. Astrophys.*, **120**, 249.
Phillips, M. M., Turtle, A. J., Edmunds, M. G. & Pagel, B. E. J., 1983. *Mon. Not. R. astr. Soc.*, **203**, 759.
Phillips, M. M., Pagel, B. E. J., Edmunds, M. G. & Díaz, A. I., 1984. *Mon. Not. R. astr. Soc.*, **210**, 701.
Sandage, A. & Brucato, R., 1979. *Astr. J.*, **84**, 472.
Sérsic, J. L. & Pastoriza, M. G., 1965. *Publs astr. Soc. Pacif.*, **77**, 287.

Shobbrook, R. R., 1966. *Mon. Not. R. astr. Soc.*, **131**, 351.
Shull, J. M. & McKee, C. E., 1979. *Astrophys. J.*, **227**, 131.
Stasińska, G., 1984a. *Astr. Astrophys. Suppl.*, **55**, 15.
Stasińska, G., 1984b. *Astr. Astrophys.*, **135**, 341.
Stauffer, J. R., 1982. *Astrophys. J.*, **262**, 66.
Stone, R. P. S. & Baldwin, J. A., 1983. *Mon. Not. R. astr. Soc.*, **204**, 347.
Terlevich, R. & Melnick, J., 1984. *Mon. Not. R. astr. Soc.*, in press.
Véron, M. P., Véron, P. & Zuiderwijk, E. J., 1981. *Astr. Astrophys.*, **98**, 34.
Ward, M. J. & Morris, S. L., 1984. *Mon. Not. R. astr. Soc.*, **207**, 867.
Ward, M. J., Penston, M. V., Blades, J. C. & Turtle, A. J., 1980. *Mon. Not. R. astr. Soc.*, **193**, 563.
Wolstencroft, R. D., Perley, R. & Tully, R. B., 1984. *Mon. Not. R. astr. Soc.*, **207**, 889.
Wright, A. E., Savage, A. & Bolton, J. G., 1977. *Aust. J. Phys. Astrophys. Suppl.*, **41**, 1.